J Mol Model (2006) 12: 665–672
DOI 10.1007/s00894-005-0021-y

ORIGINAL PAPER

Yirong Mo

Probing the nature of hydrogen bonds in DNA base pairs

Received: 2 May 2005 / Accepted: 27 June 2005 / Published online: 6 May 2006

Abstract Energy decomposition analyses based on the block-localized wave-function (BLW-ED) method are conducted to explore the nature of the hydrogen bonds in DNA base pairs in terms of deformation, Heitler–London, polarization, electron-transfer and dispersion-energy terms, where the Heitler–London energy term is composed of electrostatic and Pauli-exchange interactions. A modest electron-transfer effect is found in the Watson–Crick adenine–thymine (AT), guanine–cytosine (GC) and Hoogsteen adenine-thymine (H-AT) pairs, confirming the weak covalence in the hydrogen bonds. The electrostatic attraction and polarization effects account for most of the binding energies, particularly in the GC pair. Both theoretical and experimental data show that the GC pair has a binding energy (−25.4 kcal mol^{-1} at the MP2/6-31G** level) twice that of the AT (−12.4 kcal mol^{-1}) and H-AT (−12.8 kcal mol^{-1}) pairs, compared with three conventional N-H···O(N) hydrogen bonds in the GC pair and two in the AT or H-AT pair. Although the remarkably strong binding between the guanine and cytosine bases benefits from the opposite orientations of the dipole moments in these two bases assisted by the π-electron delocalization from the amine groups to the carbonyl groups, model calculations demonstrate that π-resonance has very limited influence on the covalence of the hydrogen bonds. Thus, the often adopted terminology "resonance-assisted hydrogen bonding (RHAB)" may be replaced with "resonance-assisted binding" which highlights the electrostatic rather than electron-transfer nature of the enhanced stabilization, as hydrogen bonds are usually regarded as weak covalent bonds.

Keywords Hydrogen bond · DNA base pair · Charge transfer · Electrostatic interaction · Resonance-assisted hydrogen bonding (RAHB)

Introduction

Molecular simulations of biological systems and computational high-throughput screening of drug candidates rely heavily on the quality of force fields, where the potential-energy function is generally expressed as the summation of various bonded and nonbonded energy terms [1–3]. However, there are few straightforward experimental proofs to justify the formulations and magnitudes of these energy terms. Only theoretical studies can provide valuable insights into the interatomic and intermolecular interactions pivotal for the development of next-generation force fields. In particular, force-field formulations and parameterizations may be monitored and refined by intermolecular interaction-energy decomposition analyses [4–11]. For instance, it has been shown that a simple electrostatic model works impressively well for strong noncovalent cation–π interactions [12–15], which play a key role in biological recognition. On the other hand, recent work shows that the polarization effect is comparable to the magnitude of electrostatic interactions [16] and consequently a polarizable force field is necessary to model cation–π interactions [17]. This dilemma was resolved by our recent energy-decomposition analyses on a series of cation–π complexes, where the results show that electrostatic, polarization and charge-transfer energy terms have good linear relationships with the total interaction energies [18]. This finding indicates that if the electrostatic energy is scaled in a way that the final interaction energies are close to the experimental or high-level quantum mechanical results, even simple force fields without explicit polarization and charge-transfer terms can model cation–π complexes very successfully.

Similarly, it has also been conceived for a long time that the hydrogen bonds in the DNA base pairs are

Dedicated to Professor Paul von Ragué Schleyer on the occasion of his 75th birthday

Y. Mo
Department of Chemistry, Western Michigan University, Kalamazoo, MI, 49008 USA
E-mail: yirong.mo@wmich.edu

basically electrostatic in nature [19–21] since nonpolarizable force fields have been extensively applied to simulate DNA interactions and transitions [22, 23], although this notion is somewhat counterintuitive to the concept of covalence in hydrogen bonds. Indeed, recent work by Bickelhaupt and collaborators [24–26] revealed that the charge-transfer between the lone pairs on oxygen or nitrogen to the N–H σ-antibonds in the Watson–Crick (WC) pairs are of comparable strength as electrostatic interactions based on density functional theory. Because of the significance of this new point of view in the development of force fields for molecular dynamics simulations of nucleic acids and proteins, here I have probed the nature of the hydrogen bonds in the WC adenine–thymine (AT) and guanine-cytosine (GC) base pairs using the recently proposed block-localized wavefunction energy decomposition (BLW-ED) method [11, 27]. In addition, parallel DNAs have been found in some hairpins and linear DNAs, and parallel stranded DNA has been detected in specific chromosome regions. Instead of the WC hydrogen bond (H-bond) pairing, parallel stranded DNAs may adopt the Hoogsteen (H) hydrogen-bond pattern [28], whereas further detailed molecular dynamics simulations revealed that actually many structures may coexist in the gas phase [23]. Thus, a Hoogsteen adenine–thymine (H-AT) base pair will also be investigated in this work. An attractive characteristic of the present BLW-ED method in comparison with other energy-decomposition schemes is the construction of an intermediate diabatic state where charge transfer among interacting monomers is quenched and the wavefunction is self-consistently optimized. This kind of intermediate diabatic state corresponds to a resonance structure (often the most stable) within conventional resonance theory. In such a way, a physical separation of polarization and charge-transfer effects and exploration of the charge-transfer effect on geometry, energy, charge redistribution etc. are feasible. It is also worthwhile to point out that most energy-decomposition schemes are based on the analysis of an adiabatic state wavefunction. In our BLW-ED method, basis set superposition error (BSSE) [29] is included in the computational algorithm and attributed to the CT energy [11]. The method has been applied to a variety of systems, including cation–π and acid–base complexes, and has shown trivial basis set dependence from 6-31G* to 6-311 + G** and cc-pVTZ [18, 30, 31].

Computational methods

In the BLW-ED method, the binding energy ΔE_B at the Hartree–Fock (HF) level between two monomers A and B is defined as the sum of deformation energy ΔE_{def} consumed to deform the monomers from their isolated optimal structures to the geometries in the energy-minimum state of dimer AB, and the intermolecular interaction energy ΔE_{int}

$$\Delta E_B(\mathrm{HF}) = \Delta E_{def} + \Delta E_{int} \tag{1}$$

The latter is the energy variation of the dimer (whose wavefunction is Ψ_{AB}) relative to the sum of the individual energies of monomers (whose wavefunctions are $\Psi^0{}_A$ and $\Psi^0{}_B$) with a correction for the BSSE [29] and is further decomposed into the Heitler–London energy (ΔE_{HL}), polarization energy (ΔE_{pol}) and charge-transfer energy (ΔE_{CT}) terms

$$\begin{aligned}\Delta E_{int} &= E(\Psi_{AB}) - E(\Psi^0_A) - E(\Psi^0_B) + \mathrm{BSSE} \\ &= \Delta E_{HL} + \Delta E_{pol} + \Delta E_{CT}\end{aligned} \tag{2}$$

The derivation of these individual energy terms is based on the construction of the initial block-localized wavefunction for the dimer Ψ^{BLW0}_{AB} as well as its self-consistent form Ψ^{BLW}_{AB} as

$$\Psi^{BLW0}_{AB} = \hat{A}(\Psi^0_A \Psi^0_B) \tag{3a}$$

$$\Psi^{BLW}_{AB} = \hat{A}(\Psi_A \Psi_B) \tag{3b}$$

In a BLW as Eq. 3, the orbitals belonging to either monomer A or B are constrained to be mutually orthogonal, as in conventional MO methods, while those belonging to different monomers are nonorthogonal, as in VB methods. The self-consistent optimization of the block-localized orbitals in Eq. 3b can be accomplished using successive Jacobi rotation as initially adopted [27], or using Gianinetti et al.'s algorithm [32, 33]. Of significance, Gianinetti and coworkers demonstrated that the self-consistent-field solution of a wavefunction like BLW can be decomposed to coupled Roothaan-like equations and each equation corresponds to a monomer. As a consequence, the overall computational cost for the BLW method is reduced and becomes comparable to the HF method.

With the above definitions of initial and optimal BLWs in Eq. 3, the energy terms in Eq. 2 can subsequently be expressed as

$$\Delta E_{HL} = E(\Psi^{BLW0}_{AB}) - E(\Psi^0_A) - E(\Psi^0_B) \tag{4a}$$

$$\Delta E_{pol} = E(\Psi^{BLW}_{AB}) - E(\Psi^{BLW0}_{AB}) \tag{4b}$$

$$\Delta E_{CT} = E(\Psi^{HF}_{AB}) - E(\Psi^{BLW}_{AB}) + \mathrm{BSSE} \tag{4c}$$

The Heitler–London energy (Eq. 4a) is defined as the energy change by bringing monomers together without disturbing their individual electron densities, while the polarization energy (Eq. 4b) corresponds to the stabilization of the complex due to the mutual relaxation of individual electron densities. In this polarization step, however, there is no penetration of electrons between two monomers. The extension of electron movements from block-localized orbitals to the whole complex further stabilizes the complex and this energy variation is denoted as the charge-transfer energy (Eq. 4c). In this step, the BSSE is also introduced, thus the correction is completely assigned to the charge-transfer energy term. It should be noted that ΔE_{HL} is a sum of electrostatic

and Pauli-exchange repulsion energies. Since the exchange of electrons is a quantum-mechanical effect and classical force-field approaches have difficulties to formulate the exchange energy separately, here I simply use ΔE_{HL}. This also enables us to port the BLW code to GAMESS to make use of the existing direct SCF codes [34]. In Eq. 3b, the optimization of Ψ_{AB}^{BLW},where the orbitals in Ψ_A or Ψ_B are orthogonal and the orbitals between Ψ_A and Ψ_B are nonorthogonal, comprises the major task of the BLW calculations [11, 27]. The electron correlation contribution ΔE_{cor}, which is mostly responsible for the dispersion phenomenon, can be estimated by the comparison between the interaction energies calculated at the HF level and higher levels (in this work the MP2 level is employed). Overall, the binding energy ΔE_B is decomposed into deformation energy (ΔE_{def}), Heitler–London energy (ΔE_{HL}), polarization energy (ΔE_{pol}), charge-transfer energy (ΔE_{CT}) and correlation energy (ΔE_{cor}) terms as

$$\Delta E_B(\mathrm{MP2}) = \Delta E_{def} + \Delta E_{HL} + \Delta E_{pol} + \Delta E_{CT} + \Delta E_{cor}(\mathrm{MP2}) \quad (5)$$

Results and discussion

At first I optimized the geometries of WC–AT and GC base pairs, as well as Hoogsteen AT (H-AT) pair, as shown in Fig. 1, and their monomers at the MP2 level with both the 6-31G* and 6-31G** basis sets, using the Gaussian98 computer program [35]. Table 1 lists the optimal hydrogen-bond lengths in the base pairs, compared with available data in the literature. The general survey of Table 1 confirms the importance of electron correlation to the geometries, which seems a general rule for hydrogen-bonding systems due to the flat energy surface around the energy-minimum states. With the same basis set (6-31G**), optimizations at both B3LYP and MP2 levels lead to very similar geometries for the WC base pairs. While theory seems to reproduce the hydrogen-bond lengths in the AT pair, discrepancies between theoretical prediction and experimental values in the GC pair are obvious for the N_4–O_6 and O_2–N_2 bond lengths. These discrepancies result from the fact that the experimental data are from the X-ray crystallography, and molecular environments will impose their effect on the base-pair geometries, as Guerra and Bickelhaupt [24] and Guerra et al. [25, 26] have analyzed extensively. Notably, recent studies by Šponer et al. with large basis sets reveal a significant basis-set effect on the geometries and the hydrogen-bond lengths optimized at the RI-MP2/cc-pVTZ level are much shorter than the crystal-structural data and computational results at either MP2/6-311G** or HF/cc-pVTZ levels, suggesting a larger dispersion effect in the DNA base pairs than previously thought [21].

To gain insight into the nature of the hydrogen bonds in DNA base pairs, I conducted detailed energy-decomposition analyses based on the MP2/6-31G** optimal geometries. Three different basis sets, including 6-31G*, 6-31G** and 6-311+G**, albeit small compared with Šponer et al.'s recent work [21], were employed to examine the basis-set dependency. The energetic data are compiled in Table 2. In general, it was found that all energy terms are stable with the basis sets and the total binding energies are very close to most of the other theoretical results in the literature [25, 36, 37], but about 2–3 kcal mol^{-1} lower than the aDZ → aTZ Helgaker's extrapolated binding energies due to the underestimation of dispersion energy with small basis sets [21]. Notably, the binding energy of the GC pair (−25.2 kcal mol^{-1} with the 6-311+G** basis set, compared with Šponer et al.'s −27.5 kcal mol^{-1}) is about twice as high as that of the AT (−12.2 kcal mol^{-1}, compared with Šponer et al.'s −15.0 kcal mol^{-1}) or H-AT pairs (−12.4 kcal mol^{-1}), whereas the AT and

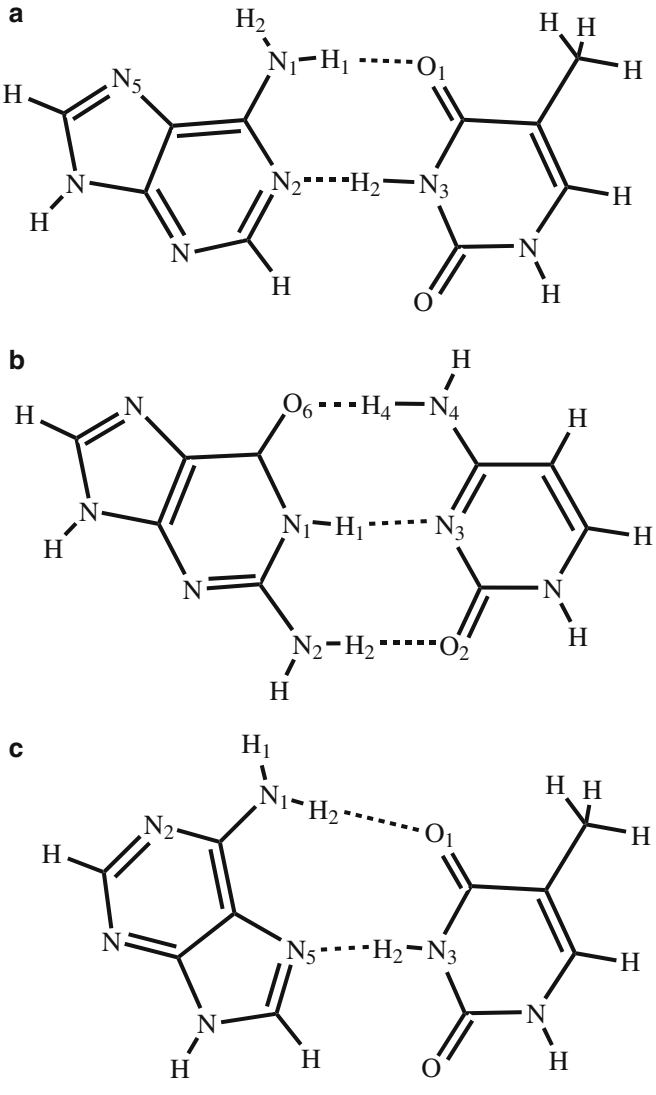

Fig. 1 Geometries of, **a** Watson–Crick ademine–thymine (WC–AT), **b** Watson–Crick guanine–cytosine (WC–GC) and **c** Hoogsteen ademine–thymine (H-AT) base pairs

Table 1 Comparison of the hydrogen-bond lengths (Å) in the DNA base pairs

Level of theory	WC–AT		WC–GC			H–AT	
	$R(N_1\_O_1)$	$R(N_2\_N_3)$	$R(O_6\_N_4)$	$R(N_1\_N_3)$	$R(N_2\_O_2)$	$R(N_1\_O_1)$	$R(N_5N_3)$–
HF/6-31G**[a]	3.09	2.99	2.92	3.04	3.02	–	–
HF/cc-pVTZ(-f)[b]	3.06	2.92	2.83	2.95	2.92	–	–
BP86/TZ2P[c]	2.85	2.81	2.73	2.88	2.87	–	–
B3LYP/6-31G**[d]	2.94	2.84	2.79	2.93	2.92	–	–
MP2/6-31G*	2.99	2.88	2.84	2.97	2.95	3.03	2.84
MP2/6-31G**	2.97	2.84	2.81	2.94	2.93	3.01	2.81
RI-MP2/cc-pVTZ[e]	2.86	2.83	2.75	2.90	2.89	–	–
X-ray[f]	2.95	2.82	2.91	2.95	2.86	–	–

[a]Šponer et al. [53, 54].
[b]Brameld et al. [37].
[c]Guerra et al. [25].
[d]Bertran et al. [36].
[e]Šponer et al. [21].
[f]Saenger [55].

H-AT pairs have similar binding energies. Since there are three regular N–H···O(N) hydrogen bonds in the GC pair, compared with two in the AT and H-AT pairs, it is intriguing to explore the nature of the very high-binding energy in the GC pair. Examination of individual energy contributions reveals that the correlation energy term is comparable in all systems, indicating that the dispersion force plays the same role in all base pairs. Moreover, although both the deformation and charge-transfer energy terms do show differences between the GC and AT or H-AT pairs, their variations are small. Remarkable discrepancies are found in the Heitler–London and polarization-energy terms. Strong electrostatic attraction and polarization effects are observed in the GC pair. Apparently, this stems from the favorable dipole–dipole electrostatic interaction between the guanine and cytosine bases, as widely recognized [21]. As the amine group is a π electron-donor group while the carbonyl group is a π electron-acceptor group, guanine and cytosine exhibit opposite dipole moments in the interfacial region, which as a result significantly stabilize the complex via classical electrostatic interaction. In contrast, such a favorable dipole–dipole interaction does not exist in the AT and H-AT pairs. The enhanced binding in the GC pair due to the stabilizing electrostatic interaction and polarization induced by π-electron resonance seems in accord with the definition of resonance-assisted hydrogen bonding (RAHB). RAHB was proposed to explain some abnormally strong intra- or intermolecular hydrogen bonds in π-conjugated systems [38–43]. In both guanine and cytosine, the π-electron resonance from the amine groups to the carbonyl groups may make the proton acceptor (carbonyl oxygen) more negative and the proton donor (amine nitrogen) more positive. On one hand, this can potentially reinforce the N–H···O hydrogen bonds as the proton acceptor can donate more electrons to the proton donor. On the other hand, since the π-electron delocalization in the guanine and cytosine bases occurs in anti-parallel directions, the binding between the guanine and cytosine is significantly enhanced due to the resonance-induced dipole moments.

Similar to Lewis acid–base complexes, the covalence in hydrogen bonds can be measured by the magnitude of the charge-transfer effect as the bond is formed by the interaction between an occupied donor orbital and virtual acceptor orbital. However, unlike strong Lewis acid–base complexes such as BH_3NH_3, where the charge-transfer energy is comparable to the overall interaction energy [30, 31, 44], in DNA base pairs I observed a relatively weak charge-transfer interaction, which accounts for around 20–35% of the overall interaction (excluding the structural deformation energy and note the Pauli repulsion largely offset the electrostatic attraction). This indicates a low covalence in the hydrogen bonds. Interestingly, as there are two hydrogen bonds in the AT and H-AT pairs but three hydrogen bonds in the GC pair, the charge-transfer stabilization energy is roughly proportional to the number of hydrogen bonds. This linear correlation will be improved further if the very weak C–H···O = C hydrogen bonding is taken into account (see below). It is also noted that in Guerra et al.'s analyses, the orbital-interaction energy term (ΔE_{oi}) is essentially a sum of the polarization, charge-transfer and dispersion energies in our approach [24–26]. Among these three components, only the charge-transfer term reflects the strength of covalence in hydrogen bonds. The polarization effect, which is induced by the mutual influence of two monomers, essentially has an electrostatic origin. Thus, our current analyses show that, although there is indeed some covalence nature in the hydrogen bonds in DNA base pairs, much of the binding energies come from the electrostatic attraction, particularly in the GC pair.

Conventionally, the bonding nature in DNA base pairs can be illustrated by the frontier orbitals (HOMO's and LUMO's) of individual bases [25]. Alternatively, we can plot electron density difference (EDD) maps, which can intuitively demonstrate the electron movement due to either the polarization or charge-transfer effects. Since the BLW defines a diabatic state where the electron flow among monomers is forbidden, the difference between the electron densities of the delocalized HF wavefunction Ψ_{AB} and optimal BLW Ψ_{AB}^{BLW} uniquely highlights the electron transfer between the monomers A and B. On the other hand, the polarization effect can be visualized by the electron-density difference between Ψ_{AB}^{BLW} and Ψ_{AB}^{BLW0}.

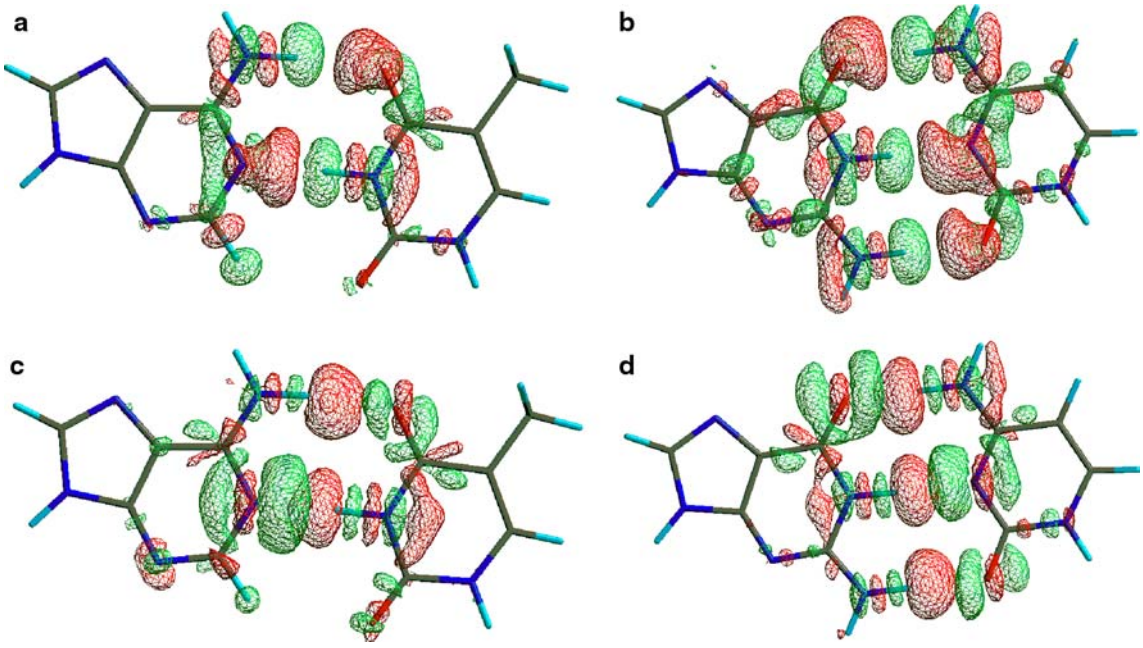

Fig. 2 Electron density difference (EDD) maps: **a** and **b** show the polarization effect in the AT and GC pairs (isodensity 1.2×10^{-3} a.u.); **c** and **d** show the charge transfer effect in AT and GC (isodensity 2×10^{-4} a.u.)

Figure 2 shows the polarization and charge-transfer effects in AT and GC pairs, where the red denotes the gain of electron density while green means the loss of electron density. In the interface between adenine and thymine or guanine and cytosine, N–H bond polarization from hydrogen to nitrogen in all monomers is observed (Fig. 2a, b), whereas hydrogen-bond acceptors gain electron density from adjacent atoms to prepare for the formation of hydrogen bonds, which makes these acceptors lose electron density to the proton donors (Fig. 2c, d). However, I find that both the polarization and charge-transfer effects are mostly local, indicating the secondary role of the π-aromatic rings in the hydrogen bonding in the DNA base pairs. The only exception is the polarization in the GC pair (Fig. 2b), where I see a small polarization involving the aromatic rings in the guanine and cytosine bases. With the formation of hydrogen bonds, proton acceptors lose electron density to the opposite protons. This confirms the sort of covalent nature of the hydrogen bonds in the DNA base pairs.

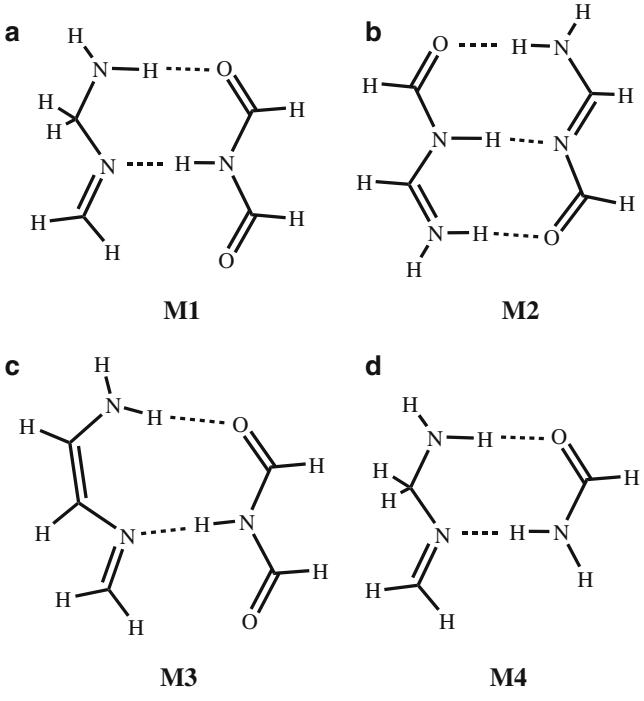

Fig. 3 Geometries of simplified models to simulate the interactions in, WC–AT **a** Watson–Crick guanine–cytosine, **b** and Hoogsteen adenine–thymine, **c** base pairs. **d** is a further simplified model of **a** by removing the carbonyl group in the right side

To verify our above claim that the hydrogen-bonding in the DNA base pairs is mostly due to the local polarization as well as favorable electrostatic interactions further, I designed three simplified models, M1, M2 and M3, to mimic the interactions in the AT, GC and H-AT pairs by retaining only the interfacial parts with unchanged structural parameters as shown in Fig. 3. Similarly, BLW-ED analyses on these systems were conducted and the results are listed in Table 3 (note here the total interaction energy ΔE_{int} does not consider the deformation energy). Comparison of the energy terms in these simplified models with those of complete DNA pairs reveals interesting information. Firstly, it is found that the dispersion energy loses about 1 kcal mol^{-1} in all simplified models. Secondly, the charge transfer effect has little change in the AT and H-AT pairs, but reduces by about 0.5 kcal mol^{-1} in the GC pair. This indicates that the covalence in the hydrogen

Table 2 Energy contributions to the binding energies in nucleic acid base pairs (kcal mol^{-1})[a]

Energy term	6-31G*			6-31G**			6-311+G**		
	WC–AT	WC–GC	H–AT	WC–AT	WC–GC	H–AT	WC–AT	WC–GC	H–AT
Deformation energy (ΔE_{def})	2.5	4.4	2.3	2.5	4.4	2.2	2.6	4.4	2.2
Heitler–London energy (ΔE_{HL})	−1.4	−10.9	−2.4	−1.7	−11.2	−2.7	0.0	-9.0	−1.0
Polarization energy (ΔE_{pol})	−5.2	−10.4	−4.9	−5.2	−10.4	−4.9	−5.9	−11.1	−5.7
Charge-transfer energy (ΔE_{ct})	−4.1	−5.5	−3.9	−4.3	−5.6	−4.1	−4.8	−6.1	−4.6
Dispersion energy (ΔE_{corr})	−3.8	−3.1	−3.7	−3.7	−2.6	−3.3	−4.1	−3.4	−3.3
Binding energy (ΔE_B)	−12.0	−25.4	−12.6	−12.4	−25.4	−12.8	−12.2	−25.2	−12.4

[a]Structural parameters are based on the optimal geometries at the MP2/6-31G(d,p) level.

Table 3 Energy contributions to the interaction energy in reduced model systems (kcal mol^{-1})[a]

Energy term	6-31G*				6-31G**				6-311+G**			
	M1	M2	M3	M4	M1	M2	M3	M4	M1	M2	M3	M4
ΔE_{HL}	1.0	-3.5	0.4	3.4	0.7	-3.7	0.2	3.2	2.4	-1.5	1.8	5.1
ΔE_{pol}	−4.6	−8.8	−4.8	−4.3	−4.6	−8.8	−4.8	−4.3	−5.2	−9.4	−5.4	−4.9
ΔE_{ct}	−4.1	−5.1	−4.0	−3.6	−4.2	−5.2	−4.2	−3.8	−4.8	−5.6	−4.8	−4.3
ΔE_{corr}	−2.5	−2.3	−2.9	−2.5	−2.6	−2.4	−3.0	−2.7	−2.7	−2.5	−3.1	−3.0
ΔE_{int}	−10.2	−19.7	−11.3	−7.0	−10.7	−20.1	−11.8	−7.6	−10.3	−19.0	−11.6	−7.1

[a]Structural parameters are based on the optimal geometries of DNA base pairs at the MP2/6-31G** level.

bonds changes only slightly. Thirdly, the polarization effect reduces slightly in the AT and H-AT pairs (less than 0.6 kcal mol^{-1}), but a modest reduction is observed in the GC pair (about 2 kcal mol^{-1}). This echoes the finding in the EDD map (Fig. 2b), which suggests a slight involvement of aromatic rings in the polarization of the GC pair. Finally, the biggest impact by removing the aromatic rings in the DNA pairs is the reduction of the electrostatic attractions. Table. 2 and 3 show that there are 2.4 and 2.8 kcal mol^{-1} reductions in the Heitler–London energies for the AT and H-AT pairs. In contrast, for the GC pair, the reduction is as high as 7.5 kcal mol^{-1}. Since Pauli-exchange repulsion decays more quickly (in exponential function [31]) than the electrostatic interaction and the binding regions are unchanged in the simplified model, I reckon that these energy changes are completely due to the reduction of electrostatic attractions. In this sense, I feel that the nature of RAHB is actually the resonance-enhanced electrostatic attraction and polarization effect, as the covalence in hydrogen bonds has only slight changes. To confirm this claim, we can further analyze individual hydrogen bonds in DNA base pairs with simple models, such as those shown in Scheme 1 for the AT pair, where the hydrogen bond lengths and orientations retain as in the base pair. With the 6-311+G** basis set, I computed the charge-transfer energies in the N–H···O and N···H–N hydrogen bonds which are −0.7 and −2.8 kcal mol^{-1}, respectively. The low value in the N-H···O bond may originate from the longer bond distance (2.97 Å) than the N···H–N bond (2.84 Å). Nevertheless, the sum of the charge-transfer energies in these two simple models without any resonance assistance (−3.5 kcal mol^{-1}) accounts for most of the charge-transfer stabilization energy in the AT base pair (−4.8 kcal mol^{-1}), indicating the limited enhancement of the hydrogen bond strength due to the resonance (Scheme 1).

The possible role of the C–H···O=C hydrogen bond in biological structures and functions has been widely discussed [45–52], primarily due to the large number of this kind of bonds in biosystems. To investigate the C–H···O=C hydrogen bond in the AT pair, I further removed the carbonyl group in model M1 to generate model M4, as shown in Fig. 3d. The results of the subsequent energy decomposition analysis of M4 are also listed in Table 3. Compared with model M1, once again the largest energetic change comes from the electrostatic interaction, which accounts for around 2.5 kcal mol^{-1} of 3.2 kcal mol^{-1} reduction in the total interaction. The removal of the carbonyl group reduces the electron-transfer stabilization by 10%, suggesting extremely weak covalence in C–H···O=C hydrogen bonding, whose interaction is dominated by the electrostatic forces. Here the allocation of a small fraction of the charge-transfer energy to the C–H···O=C hydrogen bond further legi-

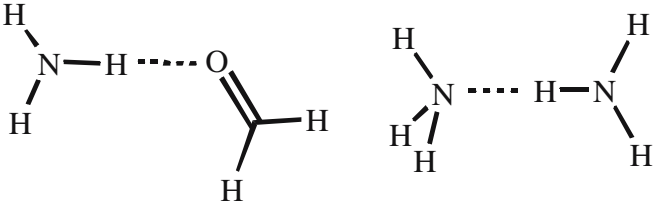

Scheme 1 Individual models for the H-bonds in the AT pair

timates our claim that the RAHB is of the electrostatic rather than charge-transfer nature.

Conclusion

There have been controversies regarding the nature of hydrogen bonds. While all experimental and theoretical studies confirm the directionality of hydrogen bonds, in accord with the definition of covalent bonds, a widespread belief is that hydrogen bonds are predominantly electrostatic in nature. The present studies of the DNA base pairs show a modest charge-transfer effect between pairing bases, and the charge-transfer stabilization accounts for only 20–35% of the overall interaction energy, while both the electrostatic (which is largely cancelled out by the Pauli-exchange interaction) and polarization energies play larger roles than the charge-transfer effect in the binding of base pairs, notably in the GC pair. This suggests a low covalence in the hydrogen bonds. Guerra et al.'s recent work, however, concluded a much more significant role of the electron-transfer effect in the DNA base pair than previous and current analyses and they found that donor-acceptor orbital interactions (i.e. charge transfer) is of the same order of magnitude as the electrostatic interaction term [24, 25, 26]. However, it should be noted that the orbital-interaction energy term in their analyses is composed of both the polarization and charge-transfer effects, and the former is of electrostatic origin.

Further analyses show that the strong binding in the GC results from favorable dipole-dipole electrostatic interaction between the guanine and cytosine bases, which is assisted by the π-electron delocalization from the amine groups to the carbonyl groups in both bases (but in reversal directions). I find that the π-electron delocalization in DNA bases strengthens the hydrogen bonds very moderately, and most of the enhanced stabilization due to π-resonance comes from the electrostatic and polarization effects. As a consequence, I recommend the terminology "resonance-assisted binding" instead of "resonance-assisted hydrogen bonding (RHAB)" to emphasize the electrostatic rather than electron-transfer nature of the enhanced stabilization in DNA base pairs.

Acknowledgement This work was supported by Western Michigan University.

References

1. Burkert U, Allinger NL (1982) Molecular mechanics. American Chemical Society, Washington DC
2. Brooks BR, Bruccoleri RE, Olafson BD, States DJ, Swaminathan S, Karplus M (1983) J Comp Chem 4:187–217
3. Reindl B, Clark T, Schleyer PvR (1996) J Comp Chem 17:1406–1430
4. Kitaura K, Morokuma K (1976) Int J Quantum Chem 10:325–340
5. Stevens WJ, Fink WH (1987) Chem Phys Lett 139:15–22
6. Gutowski M, Piela L (1988) Mol Phys 64:337–355
7. Cybulski SM, Scheiner S (1990) Chem Phys Lett 166:57–64
8. Moszynski R, Heijmen TGA, Jeziorski B (1994) Mol Phys 88:741–758
9. Glendening ED, Streitwieser A (1994) J Chem Phys 100:2900–2909
10. van der Vaart A, Merz KM Jr (1999) J Phys Chem A 103:3321–3329
11. Mo Y, Gao J, Peyerimhoff SD (2000) J Chem Phys 112:5530–5538
12. Gentle IR, Ritchie GLD (1989) J Phys Chem 93:7740–7744
13. Craven IE, Hesling MR, Laver DR, Lukins PB, Ritchie GLD, Vrbancich J (1989) J Phys Chem 93:627–631
14. Dougherty DA (1996) Science 271:163–168
15. Mecozzi S, West AP, Dougherty DA (1996) J Am Chem Soc 118:2307–2308
16. Cubero E, Luque FJ, Orozco M (1998) Proc Natl Acad Sci USA 95:5976–5980
17. Caldwell JW, Kollman PA (1995) J Am Soc Chem 117:4177–4178
18. Mo Y, Subramanian G, Ferguson DM, Gao J (2002) J Am Chem Soc 124:4832–4837
19. Morokuma K (1977) Acc Chem Res 10:294–300
20. Jeffrey GA (1997) An introduction to hydrogen bonding. Oxford University Press, New York
21. Šponer J, Jurecka P, Hobza P (2004) J Am Chem Soc 126:10142–10151
22. Cheatham TE III, Kollman PA (2000) Ann Rev Phys Chem 51:435–471
23. Kratochvíl M, Šponer J, Hobza P (2000) J Am Chem Soc 122:3495–3499
24. Guerra CF, Bickelhaupt FM (1999) Angew Chem Int Ed 38:2942–2945
25. Guerra CF, Bickelhaupt FM, Snijders JG, Baerends EJ (1999) Chem Eur J 5:3581–3594
26. Guerra CF, Bickelhaupt FM, Snijders JG, Baerends EJ (2000) J Am Chem Soc 122:4117–4128
27. Mo Y, Peyerimhoff SD (1998) J Chem Phys 109:1687–1697
28. Cubero E, Luque FJ, Orozco M (2001) J Am Chem Soc 123:12018–12025
29. Boys SF, Bernardi F (1970) Mol Phys 19:553–566
30. Mo Y, Gao J (2001) J Phys Chem A 105:6530–6536
31. Mo Y, Song L, Wu W, Zhang Q (2004) J Am Chem Soc 126:3974–3982
32. Gianinetti E, Raimondi, Tornaghi E (1996) Int J Quantum Chem 60:157–166
33. Gianinetti E, Vandoni I, Famulari A, Raimondi M (1998) Adv Quantum Chem 31:251–266
34. Schmidt MW, Baldridge KK, Boatz JA, Elbert ST, Gordon MS, Jensen JJ, Koseki S, Matsunaga N, Nguyen KA, Su S, Windus TL, Dupuis M, Montgomery JA (1993) J Comput Chem 14:1347–1363
35. Frisch MJ, Trucks GW, Schlegel HB, Scuseria GE, Robb MA, Cheeseman JR, Zakrzewski VG, Montgomery JAJ, Stratmann RE, Burant JC, Dapprich S, Millam JM, Daniels AD, Kudin KN, Strain MC, Farkas O, Tomasi J, Barone V, Cossi M, Cammi R, Mennucci B, Pomelli C, Adamo C, Clifford S, Ochterski J, Petersson GA, Ayala PY, Cui Q, Morokuma K, Malick DK, Rabuck AD, Raghavachari K, Foresman JB, Cioslowski J, Ortiz JV, Baboul AG, Stefanov BB, Liu G, Liashenko A, Piskorz P, Komaromi I, Gomperts R, Martin RL, Fox DJ, Keith T, Al-Laham MA, Peng CY, Nanayakkara A, Challacombe M, Gill PMW, Johnson B, Chen W, Wong MW, Andres JL, Gonzalez C, Head-Gordon M, Replogle ES, Pople JA (1998) Gaussian 98, Ed. A.9. Gaussian Inc, Pittsburgh PA
36. Bertran J, Oliva A, Rodríguez-Santiago L, Sodupe M (1998) J Am Chem Soc 120:8159–8167

37. Brameld K, Dasgupta S, Goddard WA III (1997) J Phys Chem B 101:4851–4859
38. Gilli G, Bellucci F, Ferretti V, Bertolasi V (1989) J Am Chem Soc 111:1023–1028
39. Bertolasi V, Gilli P, Ferretti V, Gilli G (1991) J Am Chem Soc 113:4917–4925
40. Steiner T (1998) Chem Commun 411–412
41. Gilli P, Bertolasi V, Ferretti V, Gilli G (2000) J Am Chem Soc 122:10405–10417
42. Munn RW, Eckhardt CJ (2001) J Phys Chem A 105:6938–6942
43. Gilli P, Bertolasi V, Pretto L, Ferretti V, Gilli G (2004) J Am Chem Soc 126:3845–3855
44. Fiacco DL, Mo Y, Hunt SW, Ott ME, Roberts A, Leopold KR (2000) J Phys Chem A 105:484–493
45. Sutor DJ (1962) Nature 195:68–69
46. Desiraju GR, Steiner T (2001) The weak hydrogen bond in structural chemistry and biology. Oxford University Press, New York
47. Meadows ES, De Wall SL, Barbour LJ, Fronczek FR, Kim M-S, Gokel GW (2000) J Am Chem Soc 122:3325–3335
48. Senes A, Ubarretxena-Belandia I, Engelman DM (2001) Proc Natl Acad Sci USA 98:9056–9061
49. Aravinda S, Shamala N, Bandyopadhyay A, Balaram P (2003) J Am Chem Soc 125:15065–15075
50. Manikandan K, Ramakumar S (2004) Proteins 56:768–781
51. Petrella RJ, Karplus M (2004). Proteins 54:716–726
52. Guo H, Beahm RF, Guo H (2004) J Phys Chem B 108:18065–18072
53. Šponer J, Leszczynski J, Hobza P (1996) J Phys Chem 100:1965–1974
54. Šponer J, Hobza P (1998) In: Schleyer PvR (ed) Encyclopedia of computational chemistry. Wiley, New York, pp 777–789
55. Saenger W (1984) Principles of nucleic acid structure (and references therein). Springer, Berlin Heidelberg New York, pp 123–124